

## Diffraction imaging for fracture detection: synthetic case study

Alexander KLOKOV, Reda BAINA, Evgeny LANDA\*, OPERA, Pierre THORE and Issam TARRASS, TOTAL

### Summary

Identification of small scale subsurface object (such as faults, pinchouts, karsts, fractures etc.) from seismic data is based usually on in-direct characteristics of the wavefield, i.e. visual discontinuity of reflectors or presents of anisotropy. At the same time the seismic response from these structural elements is encoded in diffractions. The main difficulty to use diffracted energy is its weakness compared to the reflected one. Therefore diffractions should be separated from reflections before imaging. In this study we present procedures for reflection-diffraction separation and diffraction imaging, and illustrate the feasibility of the proposed technique on realistic models.

### Introduction

A major challenge in carbonate environments is to map heterogeneities which have a strong impact on oil and gas production. In many carbonate reservoirs matrix porosity contains the oil in place but the permeability is mainly provided by fracture corridors. In other reservoirs the oil in place is found primarily in karstic caves and conduits. Therefore the ability to detect these heterogeneities and possibly characterize their properties is essential in these environments.

Several techniques have been developed to characterize these heterogeneities by analysing the elastic signals recorded in seismic experiments. The most popular refer to equivalent medium theory and take advantage of the anisotropy of the equivalent media. The application of these methods has not been so successful and in many cases it has produced erratic results. At the same time the presence of heterogeneities in the reservoir induces a second and important effect: diffraction and scattering. The main difficulty to use diffracted energy in seismic is connected to the fact that typically diffracted energy is one or even two order of magnitude weaker than reflected one and it is not easy to distinguish diffracted events in the total wavefield. Therefore diffracted and reflected energy have to be separated before imaging.

Khaidukov et al. (2004) used different moveout properties of the waves, focused reflected waves to their imaginary source location in the pseudo-depth domain, muted it, and after defocusing got gathers where reflection events were suppressed. Taner et al. (2006) showed a possibility to separate reflections and diffractions using plane-wave constant  $p$  sections. The post-migration dip-angle domain discovered significant distinction between diffractions and reflections (Landa et al., 2008; Reshef and Landa, 2009). In this domain after migration with the correct velocity

reflections appear as concave-shaped events while diffractions are flat. In this study we propose procedures for reflection-diffraction separation and diffraction images construction, and illustrate the feasibility of the proposed technique on a realistic model.

### Reflection apex removal

In this work we discuss migrated common image gathers (CIG) in dip angle domain. As usual, summation of the CIGs produces seismic image. An image of different subsurface objects (reflectors or diffractors) is formed by that part of the corresponding event on the CIG. Since reflection event on the CIGs always has a concave shape (smile), image of this point is formed by constructive summation in a vicinity of an apex of the smile. It means that if we want to eliminate reflections on the image it is necessary to subtract part of the reflection event on the CIG which is located in a vicinity of the apex of the smile. A simple way to detect the smile apex position is to parameterize a reflection event by an apex-shifted parabola and to search for a position corresponding to the maximum semblance values for every dip angle and every depth sample. Then we pick maximum semblance value for every depth using an automatic picking procedure with regularization. Obtained curve corresponds to position of reflection apex for each depth sample. We now can destruct part of the reflection event around the apex. After summation the CIGs we obtain migrated image with strongly attenuated reflection energy. Note that due to the fact that reflections on the CIGs have a concave shape regardless of the migration velocity (Landa et al., 2008) the described procedure is efficient for even in case of inaccurate velocity model.

### Hybrid Radon transform

Unlike reflection, shape of a diffraction event on CIG depends on migration velocity accuracy. Since reflection and diffraction events have quite different shapes in the post-migrated dip-angle domain they could be separated by a hybrid Radon transform (TraD, 2002). First we define two models in the Radon domain: one describes diffraction events, the other defines reflection events. Each model is connected with the data by its pair of operators.

The shape of diffraction event in the dip angle CIG is described by the following equation (Landa et al., 2008):

$$z_i(\alpha) = \frac{\gamma \cos(\alpha_i)(\gamma \Delta x \sin(\alpha_i) + D)}{1 - \gamma^2 \sin^2(\alpha_i)}, \quad (1)$$
$$D = \sqrt{(z^2(1 - \gamma^2 \sin^2(\alpha)) + \Delta x^2)}$$

In the equation above  $z_i$  – depth of the image,  $\alpha_i$  – the current dip,  $\Delta x$  – lateral shift (distance) between a diffractor and an observation point,  $\gamma$  – characterizes migration velocity accuracy and equal to  $V_m/V$ . Using this approximation we construct a pair of the transform operators: for direct transform from the data domain  $d$  to the diffraction model domain  $m_d$ :

$$m_d(\gamma, \Delta x, z_i) = \sum_i d(\alpha_i, z = z_i(\gamma, \Delta x, \alpha_i)), \quad (2)$$

and from the diffraction model domain to the data domain:

$$d(\alpha_i, z) = \sum_{\gamma} \sum_{\Delta x} m_d(\gamma, \Delta x, z(\gamma, \Delta x, \alpha_i)), \quad (3)$$

Reflections are approximated by apex-shifted parabolas. Curvature of the parabola is limited by minimum and maximum moveout on far offset.

To define the hybrid model that best fits the data in a least-squares sense we minimize the objective function  $F$ :

$$F(m_d, m_r) = \|W_{data}(L_d m_d + L_r m_r - d)\|_2 + \varepsilon_d \|W_d m_d\|_2 + \varepsilon_r \|W_r m_r\|_2, \quad (4)$$

where  $L_d$ , and  $L_r$  are diffraction and reflection Radon operators respectively,  $m_d$ , and  $m_r$  are diffraction and reflection models in the Radon domain respectively,  $W_{data}$ ,  $W_d$  and  $W_r$  are data and model's space weights,  $\varepsilon_d$ , and  $\varepsilon_r$  are diffraction and reflection measures of sparseness respectively. To find the minimum of  $F$  we use a limited-memory quasi-Newton method (Guitton and Symes, 2003).

When the models  $m_d$ , and  $m_r$  are found we invert them separately and get two datasets, one of which contains diffraction events only and another one – reflection events.

It is important to note that this separation procedure may leave relatively strong residual reflection energy in the diffraction component of the Radon domain. It is connected to the fact that part of the energy connected to the apex area of the reflections leaks into diffraction component. This is why to separate reflection and diffraction components we use two step combination of apex removal described above and Radon separation.

### Example

To illustrate application of our method we constructed a realistic synthetic model inserting a set of scatterers in a finely layered model (Figure 1). The model is built from a real well log data up-scaled at a 1m size with mild velocity variations in the upper part of the model. Three sets of scatterers, represented by a density contrast, were introduced in the density field. The first set (depth of 1125-1750 m) corresponds to a fix size set of scatterers with

decreasing density from left to right, the second (depth of 2000-2125 m) has increasing contrast (and scattering amplitude) and the third set of scatterers (depth of 2500-3000 m) has decreasing size (Figure 1).

Figure 2a shows zero-offset section of the total wavefield and Figure 2b shows the diffraction component only. Amplitudes of the diffractions are amplified 20 times for the display.

We computed dip angle CIGs from zero-offset section using the correct velocity. Figure 3a shows five dip angle CIGs. Reflection events have the form of smiles while diffractors are expected to be expressed by linear events. But they are practically invisible in the figure due to their very weak energy. Our purpose is to separate diffraction and reflection events. Firstly, we determine positions of the reflection apexes in the CIGs and mute the areas in a vicinity of the picked apex positions. In such way we eliminate the main part of the reflection energy connected to the apexes of the shifted hyperbola. At the second step we apply the hybrid Radon transform to the residual field as it is described above. Since the migration velocity in our example is correct the diffraction model was restricted to only one plane  $\gamma=1$ . The Radon transformation of a selected CIG for reflection part of the hybrid diffraction-reflection model is shown in Figure 4a. It contains only one plane for the apex shift equal to 0 (horizontal reflectors). The curvature parameter for reflection parabola was searched in the limit 3 km to 21 km. For diffraction model the lateral distance between observation point and diffractor was chosen  $\pm 500$  m. (Figure 4b).

After applying inversion of diffraction model only for every CIG we get dataset which contains mostly diffraction events. Figure 3b shows CIGs after reflection-diffraction separation. Notice that diffraction events expressed by linear events are visible now. Figure 5a shows conventional depth migration results. Results of depth imaging after wavefield separation are shown in Figure 5b. Scatterers are imaged very well.

### Conclusions

We proposed a new method for separation reflection and diffraction wavefield components in the migrated dip angle domain. This method is based on the two step procedure which contains reflection apex removal and filtering in the hybrid Radon domain. Diffraction image constructed by CIGs summation after destruction of reflection apexes has low computational cost but has relatively strong residual reflection events. This weakness can be improved by applying events separation in the hybrid Radon domain using apex-shifted parabola parameterization for reflections and analytical expression for diffractors. Application the proposed method to synthetic data illustrates potential of using diffractions for imaging of small scale elements of the subsurface. The method will be applied to real data.

## Acknowledgements

The authors thank TOTAL for supporting this research. OPERA is a private organization funded by TOTAL and supported by Pau University whose main objective is to carry out applied research in petroleum geophysics.

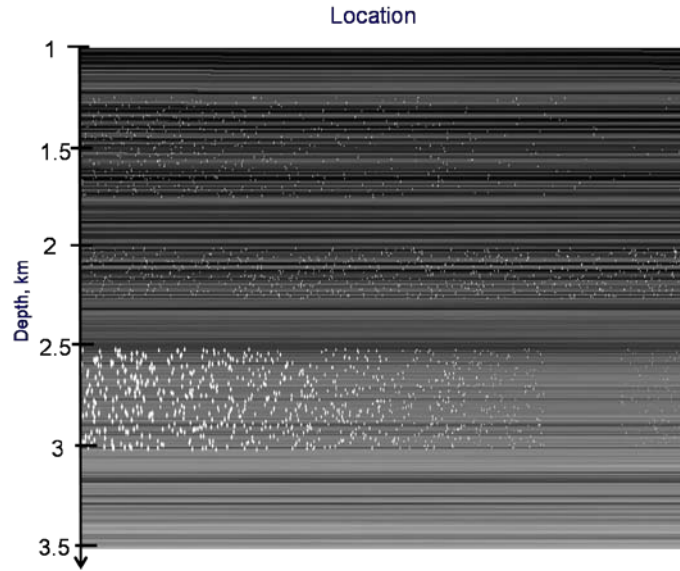


Figure 1: Synthetic model. Scatterers introduced as density contrast

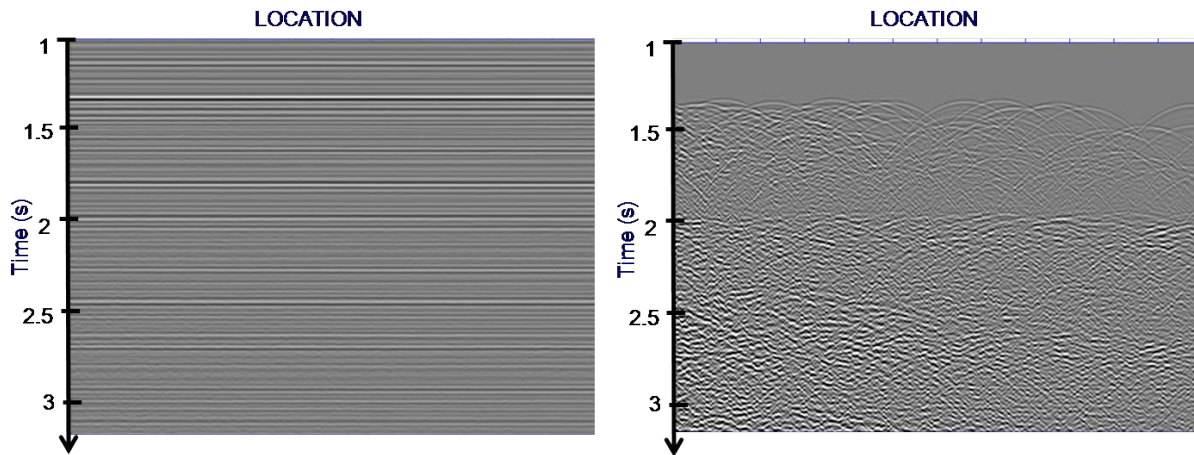


Figure 2: a) zero-offset section of the total wavefield; b) diffraction component only (20 times amplified for display).

# Diffraction imaging

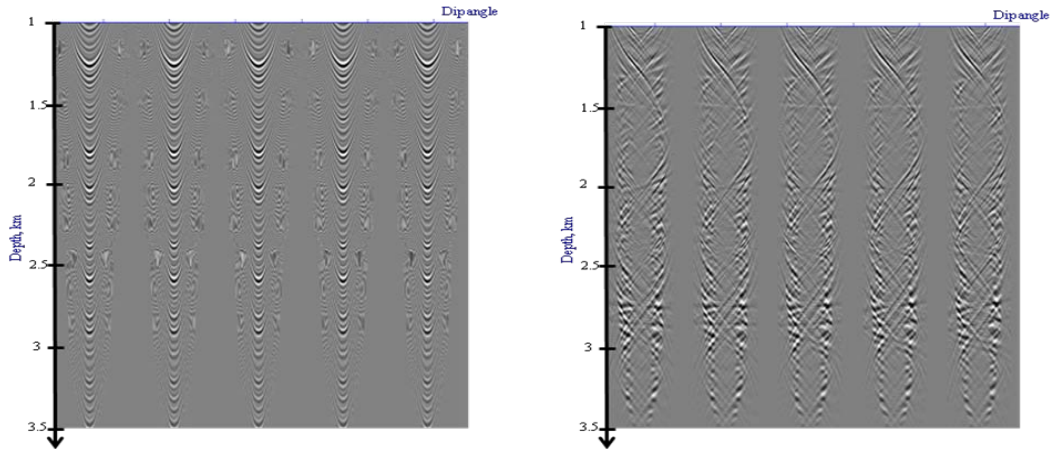


Figure 3: a) Initial CIGs; b) CIGs in dip angle domain after separation.

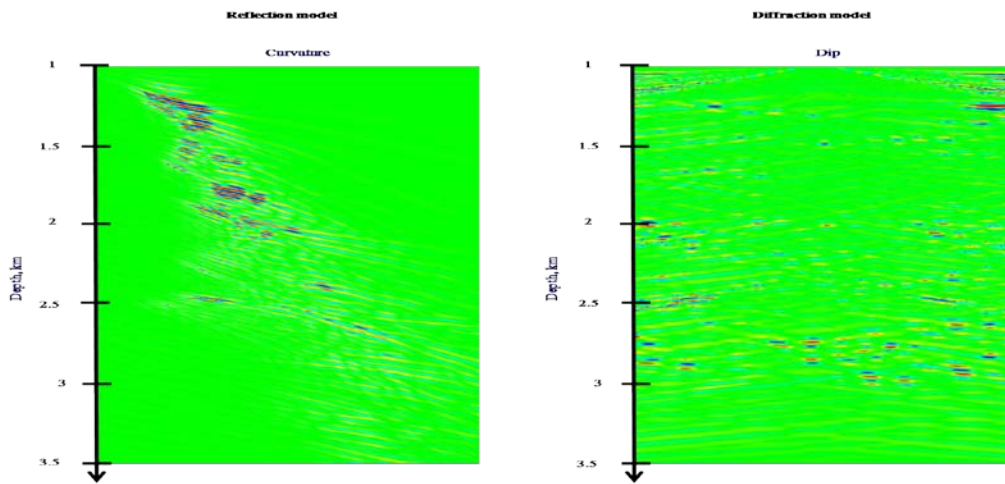


Figure 4: a) Reflections in the Radon domain; b) Diffractions in the Radon domain.

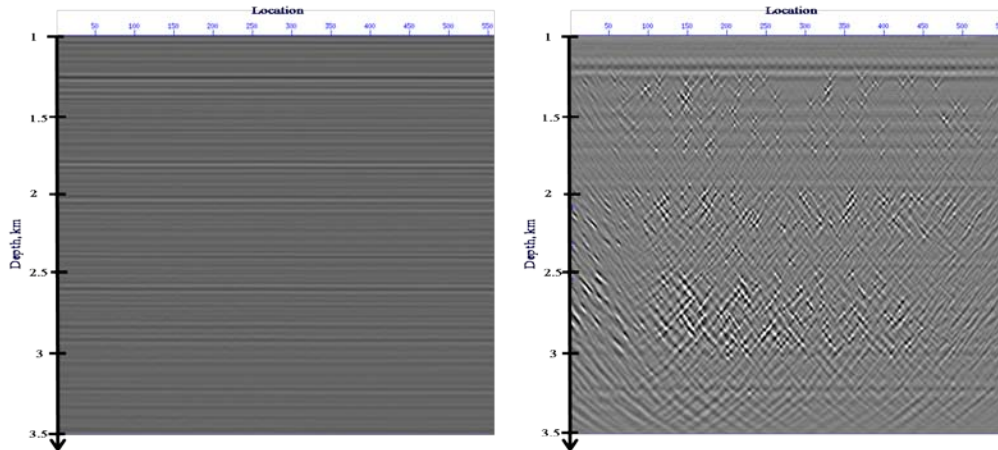


Figure 5: a) Migration of the total wavefield; b) Migration of the diffraction component of the wavefield after separation

## EDITED REFERENCES

Note: This reference list is a copy-edited version of the reference list submitted by the author. Reference lists for the 2010 SEG Technical Program Expanded Abstracts have been copy edited so that references provided with the online metadata for each paper will achieve a high degree of linking to cited sources that appear on the Web.

## REFERENCES

- Khaidukov, V., E. Landa, and T. J. Moser, 2004, Diffraction imaging by focusing-defocusing: An outlook on seismic superresolution: *Geophysics*, **69**, 1478–1490, [doi:10.1190/1.1836821](https://doi.org/10.1190/1.1836821).
- Landa, E., S. Fomel, and M. Reshef, 2008, Separation, imaging, and velocity analysis of seismic diffractions using migrated dip-angle gathers: *SEG Expanded Abstracts*, **27**, no. 1, 2176, [doi:10.1190/1.3059318](https://doi.org/10.1190/1.3059318).
- Reshef, M., 2007, Velocity analysis in the dip-angle domain: 69th EAGE meeting, Expanded Abstracts.
- Reshef, M., and E. Landa, 2009, Post-stack velocity analysis in the dip-angle domain using diffractions: *Geophysical Prospecting*, **57**, no. 5, 811–821, [doi:10.1111/j.1365-2478.2008.00773.x](https://doi.org/10.1111/j.1365-2478.2008.00773.x).
- Taner, M. T., S. Fomel, and E. Landa, 2006, Separation and imaging of seismic diffractions using plane-wave decomposition: *SEG Expanded Abstracts*, **25**, no. 1, 2401, [doi:10.1190/1.2370017](https://doi.org/10.1190/1.2370017).
- Trad, D., M. Sacchi, and T. Ulrych, 2001, A hybrid linear-hyperbolic Radon transform: *Journal of Seismic Exploration* **9**, 303–318.